V. GASEOUS ELECTRONICS

Academic and Research Staff

Prof. E. V. George   Dr. P. W. Hoff   Dr. Z. Rozwitalski
Prof. G. Bekefi   Dr. C. K. Rhodes   J. J. McCarthy
Prof. S. C. Brown   W. J. Mulligan

Graduate Students

J. L. Miller   C. W. Werner
R. H. Price   D. Wildman

A. HIGH-PRESSURE TEA CO_2 LASER

J. L. Miller

The high-pressure TEA CO_2 laser system described in Quarterly Progress Report No. 110 (pp. 59-62) has been operated at total gas pressures to 9.2 atm. Excited by a fast lumped circuit (shown in Fig. V-1) the system can be operated at repetition rates of 1 shot per 3 seconds, up to 7 atm, which furnishes laser output of ~100 mJ in 100 ns pulses.

As the gas pressure is increased, we observe several trends in the laser pulse characteristics. Pulses from high-pressure mixtures occur sooner with respect to the discharge. Figure V-2 shows that at the time after the firing of the spark gap when the laser pulse begins to rise, the pulse delay decreases from 1.3 μs to 0.7 μs as the pressure increases from 2 atm to 6.8 atm. As the pulse gets nearer in time to the discharge it also becomes narrower. In Fig. V-3 the pulse width (FWHP) is plotted as a function of pressure. At 6.8 atm the pulse width is ~100 ns.
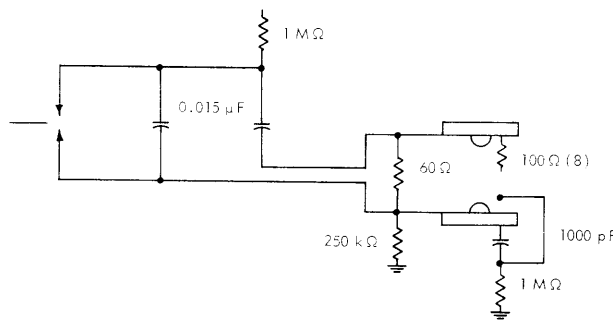

Fig. V-1. Fast lumped circuit.

In addition to these effects, as the gas pressure is raised, output appears in lines adjacent to the main laser line. Multiline operation is documented by observing the laser output simultaneously with two spectrometers (Jarrel-Ash 1/2 and 1/4 m), and
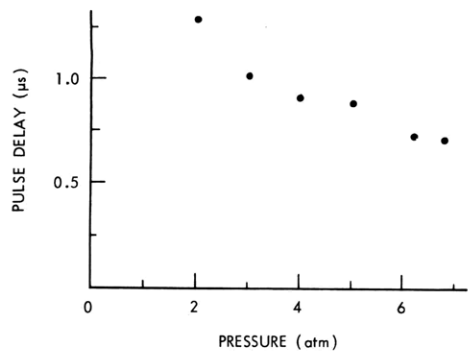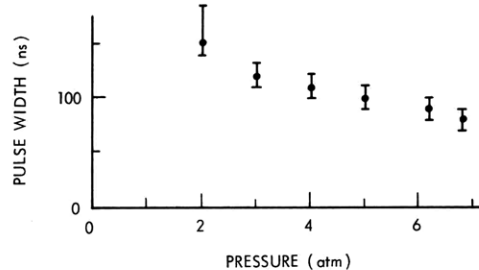
Fig. V-2. Pulse delay vs pressure.
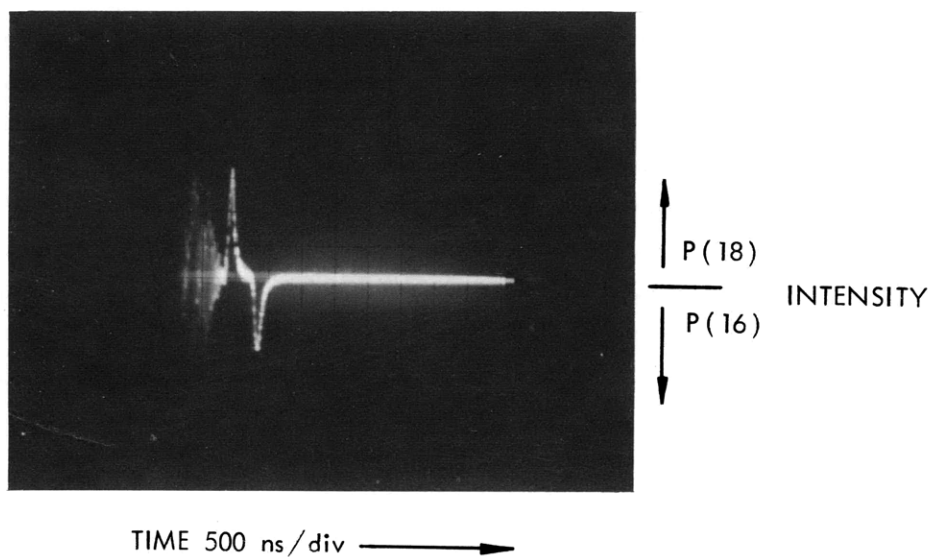

Fig. V-3. Pulse width vs pressure.

TIME 500 ns/div ⟶

Fig. V-4. Simultaneous output in P(18) and P(16) (delayed).

Table V-1. Ratio of line intensity to pressure.

Pressure (atm)	Intensity of P(18) / Intensity of P(16)	Intensity of P(18) / Intensity of P(20)
1	53	>100
3	8.0	>100
5	1.3	33

two detectors. Figure V-4 shows simultaneous operation in both the P(18) (upper pulse) and P(16) (lower pulse) lines (at 5 atm). This photograph was made by delaying the output of one of the detectors and subtracting this delayed signal from the output of the other detector, and observing with a Tektronix 7904 oscilloscope. Table V-1 shows that the ratio between the line intensities decreases as pressure is increased. A third line P(20) appears at 5 atm.

B. EVOLUTION OF FIELD IN BOUND-FREE LASER SYSTEMS

C. W. Werner

We are extending our treatment of bound-free systems to include the temporal and spectral evolution of the laser pulse. Because of the continuum nature of radiation from such a system, the theoretical treatment of field evolution must be undertaken in a somewhat different manner from that with conventional laser systems. In the frequency band of radiation, there may be several thousand axial modes, and separate consideration of each of these modes is clearly impractical. A fairly accurate description of the field development is possible if all modes in a narrow frequency band $d\nu$ are considered. In such a treatment we neglect competitive mode-mode interactions and calculate the gain of the system in the same way as we described previously,[1] except that we now employ a Morse potential for the upper state, rather than a parabolic fit to a Lennard-Jones potential.

Our procedure is as follows. Let $G(\nu)$ be the calculated gain as a function of frequency. Consider a single mode centered at frequency ν_{mode}. The rate at which the mode builds is given by

$$\frac{d\xi_\nu}{dt} = c(G(\nu) - \text{Loss})\,\xi_\nu + S(\nu),$$

where $\xi_\nu = E_\nu^2/4\pi$ is the energy per unit volume in the mode centered at ν, $S(\nu)$ is the spontaneous noise per unit volume in the mode, and the loss term takes into account the mirror and scattering losses of the cavity. $S(\nu)$ is given by the relation[2]

$$S(\nu) = \frac{\pi}{2}\,\frac{h\nu c}{\tau_{spon}}\left(\frac{\lambda}{2\pi}\right)^2 \left.\frac{dN_u}{d\nu}\right|_\nu \frac{1}{V_m},$$

where V_m is the mode volume.

The stimulated rate attributable to 1 mode is given by

$$\left(\frac{dN_u}{dt}\right)_{1\ mode} = -\frac{c}{h\nu}\,G_\nu\,\xi_\nu.$$

Summing over all modes gives the time rate of change of the upper state density

$$\frac{dN_u}{dt} = -c \sum_{modes} \frac{G(\nu)}{h\nu}\,\xi_\nu.$$

If the number of modes is large, we may replace this expression by an integral. In the frequency interval $d\nu$, there are $d\nu/(c/2L)$ modes. Hence

$$\frac{dN_u}{dt} \cong -c \int_0^\infty \frac{G(\nu)}{h\nu} \left[\frac{2L\xi(\nu)}{c}\right] d\nu,$$

where $\xi(\nu)$ is the envelope of ξ_ν. Defining an average energy density per unit frequency $F(\nu)$ given by

$$F(\nu) \equiv \frac{2L}{c}\,\xi(\nu),$$

we have

$$\frac{dN_u}{dt} = -c \int_0^\infty \frac{G(\nu)}{h\nu}\,F(\nu)\,d\nu$$

and

$$\frac{dF(\nu)}{dt} = c(G(\nu) - Loss)\,F(\nu) + \frac{h\nu}{\tau_{spon}}\left(\frac{\lambda}{2\pi}\right)^2 \frac{\pi L}{V_m} \frac{dN_u}{d\nu}.$$

We expect for a plane-plane mirror arrangement that V_m will have the form $V_m = C_m \pi r_a^2 L$, where r_a is the aperture radius, and L is the length of the cavity. C_m is a constant of order unity that takes into account the polarizations and spatial averaging of the electric field, and is unimportant in the final result. A variation of C_m over 6 orders of magnitude resulted in only a two-fold change in field magnitude. Consequently,

$$\frac{dF(\nu)}{dt} = c(G(\nu) - Loss)\,F(\nu) + \frac{1}{4\pi^2 C_m} \frac{h\nu}{\tau_{spon}}\left(\frac{\lambda}{r}\right)^2 \frac{dN_u}{d\nu}.$$

The equations in this report were solved simultaneously with the kinetic equations derived in previous reports.[1,3,4] A typical line shape is shown in Fig. V-5 for several
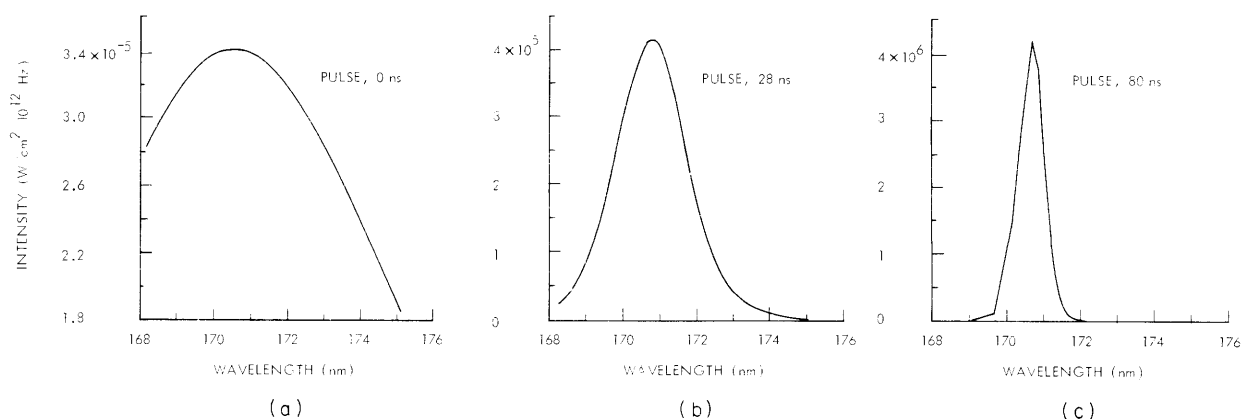
Fig. V-5. Temporal and spectral evolution of the laser pulse.
60% mirror reflectance, 20 atm xenon.

times during the laser pulse. The initial width of this line is approximately 100 Å, narrowing to ~10 Å. Experimentally, the linewidth begins at 160 Å and narrows to ~15 Å. The total intensity of the pulse integrated over frequency is shown together with the dimer density in Fig. V-6.
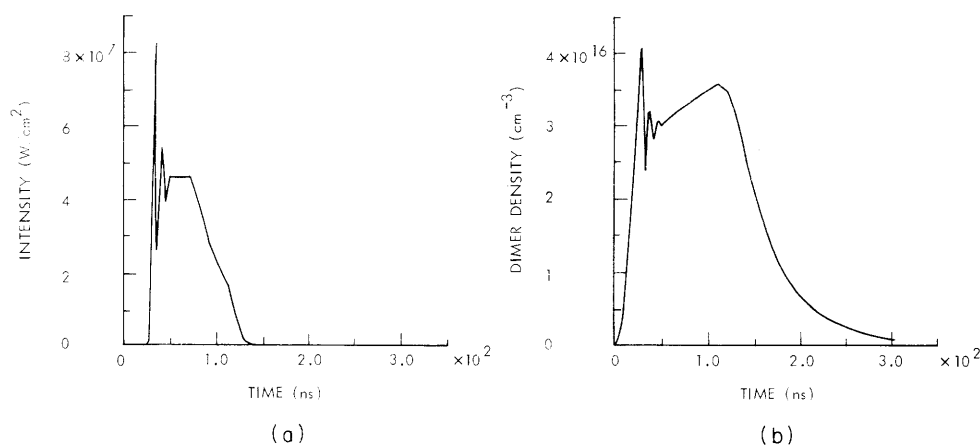
Fig. V-6. (a) Laser intensity inside cavity.
(b) Dimer density.

The "ringing" at early times is not observed experimentally and may be an artifact of the numerical integration routine, although conversely, the spikes may be too narrow to be observed experimentally. In the case illustrated, the temporal width is too large by approximately a factor of two.

Unfortunately, the results of the previous treatment are extremely sensitive to the

coefficients employed for the potential curves. The characteristics of the upper-state potential are only vaguely known. The ground-state potential is better known, but there is still some question about which exact parameters are valid. Using experimental data for the linewidth, line center, and temperature behavior of the laser, we are now attempting to fit the parameters of the potential functions. These results will be presented in a future report.

References

1. C. W. Werner, Quarterly Progress Report No. 110, Research Laboratory of Electronics, M.I.T., July 15, 1973, pp. 65-77.

2. H. A. Haus, IEEE J. Quant. Electronics, Vol. QE-1, No. 4, pp. 179-180, July 1965.

3. E. V. George and C. K. Rhodes, Quarterly Progress Report No. 109, Research Laboratory of Electronics, M.I.T., April 15, 1973, pp. 85-89.

4. C. W. Werner, Quarterly Progress Report No. 109, Research Laboratory of Electronics, M.I.T., April 15, 1973, pp. 89-95.